238
Copy
RM L56F13a

[redacted]

NACA RM L56F13a

TECH LIBRARY KAFB, NM
0144220

Rey # 1273

NACA

RESEARCH MEMORANDUM

7703

WIND-TUNNEL INVESTIGATION OF DAMPING IN ROLL AT SUPERSONIC SPEEDS OF TRIANGULAR WINGS AT ANGLES OF ATTACK

By Russell W. McDearmon and Robert A. Jones

Langley Aeronautical Laboratory
Langley Field, Va.

[redacted]

NATIONAL ADVISORY COMMITTEE
FOR AERONAUTICS
WASHINGTON
September 14, 1956

[redacted]

TECH LIBRARY KAFB, NM

0144220

NATIONAL ADVISORY COMMITTEE FOR AERONAUTICS

RESEARCH MEMORANDUM

WIND-TUNNEL INVESTIGATION OF DAMPING IN ROLL AT SUPERSONIC SPEEDS OF TRIANGULAR WINGS AT ANGLES OF ATTACK

By Russell W. McDearmon and Robert A. Jones

SUMMARY

Experimental values of the damping in roll of three triangular wings have been obtained at Mach numbers of 1.62, 1.94, 2.22, 2.41, and 2.62 over a range of angle of attack from approximately 0° to 13°. The aspect ratios of the wings were 1.46, 2.31, and 3.35.

Angle of attack had no large effect on the damping in roll for the angle-of-attack range investigated.

For all angles of attack, fairly good agreement between the experimental and theoretical damping in roll was obtained when the wing leading edges were well behind the Mach cones emanating from the wing apexes. When the leading edges were in the vicinity of the Mach cones, the damping in roll was generally overestimated by theory, this overestimation being greater for the higher angles of attack. When the leading edges were well ahead of the Mach cones, the damping in roll varied from somewhat higher than theory for the lower angles of attack to somewhat lower than theory for the higher angles of attack.

INTRODUCTION

One of the more important stability derivatives which must be evaluated in order to predict the dynamic stability characteristics of airplanes and missiles is the damping-in-roll derivative C_{l_p}. References 1 to 10 present some of the experimental and theoretical work that has been done to determine C_{l_p} at supersonic speeds both for complete airplane configurations and for isolated wings at zero angle of attack. The purpose of the present investigation was to determine the effects of angle of attack on C_{l_p} for isolated triangular wings.

The damping in roll of three sting-mounted triangular wings was obtained in the Langley 9-inch supersonic tunnel at Mach numbers of 1.62, 1.94, 2.22, 2.41, and 2.62 over a range of angle of attack from approximately 0° to 13°. The damping in roll was obtained by a forced-roll technique. The wing plan forms were selected to provide a range of leading-edge sweep angle such that the leading edges passed from behind to ahead of the Mach cones emanating from the wing apexes. The wings had aspect ratios of 1.46, 2.31, and 3.35.

SYMBOLS

The symbols used in the present paper are defined in the following list. The rolling moments are referred to the stability-axes system, with the origin at the calculated mass center of gravity of the wing.

A	aspect ratio, b^2/S
b	wing span, in.
$\beta = \sqrt{M^2 - 1}$	
C_l	rolling-moment coefficient, M_X/qSb
C_{l_p}	damping-in-roll derivative, $\partial C_l \Big/ \partial \frac{pb}{2V}$
α	angle of attack, deg
ϵ	semiapex angle of wing, deg
M_X	rolling moment about longitudinal stability axis
M	free-stream Mach number
μ	Mach angle, $\sin^{-1} \frac{1}{M}$, deg
p	angular rolling velocity, radians/sec
$pb/2V$	wing-tip helix angle, radians
q	free-stream dynamic pressure
R	Reynolds number based on mean aerodynamic chord of wing

S	wing area, sq in
V	free-stream velocity
c_r	wing root chord, in.

APPARATUS

Wind Tunnel

All tests were made in the Langley 9-inch supersonic tunnel, which is a closed-circuit, continuous-operation type of tunnel in which the stream pressure, temperature, and humidity can be controlled at all times during tunnel operation. Different test Mach numbers are provided by interchangeable nozzle blocks which form test sections approximately 9 inches square. Eleven fine-mesh turbulence-damping screens are installed in the settling chamber ahead of the supersonic nozzle. The turbulence level of the tunnel is considered low, based on past turbulence-level measurements. Throughout the tests, the moisture content in the tunnel was kept sufficiently low to insure that the effects of condensation were negligible.

Models, Support, and Rolling-Moment Balance

The pertinent wing characteristics are presented in table I. All wings were made of 1/8-inch-thick steel sheet. The leading and trailing edges of the wings were beveled symmetrically at an angle of 5° in a direction parallel to the root chord. (See sketch in table I.) A pair of wings was made for each semiapex angle; and each pair was very nearly identical, except that the center portion (portion near the root chord) of each wing of a pair was modified in a different manner to fit a different type of mounting sting.

Two types of steel mounting stings were used in the tests. The first type consisted of an ogival nose and a cylindrical afterbody, and had a longitudinal slot cut at the desired angle of attack. The wing was mounted on the sting by being inserted into the slot and secured by lock screws and pins. This type of sting was used to obtain angles of attack of approximately 0° and 3.5°. The second type of sting was cylindrical throughout its length, and the nose end was beveled at the desired angle of attack. A flat plate shaped to fit a recess in the upper wing surface was silver-soldered to the beveled surface. The wing was attached to the plate with screws. This type of sting was used to obtain angles of attack of approximately 6.7°, 9.7°, and 12.8°. Photographs of wings mounted on both types of stings are presented in figure 1.

Transition strips of aluminum-oxide particles were placed on the upper and lower surfaces near the leading edges of the wings. These strips were 1/8 inch wide and approximately 0.006 inch thick. They may be seen in the photographs of figure 1.

The exposed surfaces of the wings and stings were ground and polished to a smooth finish. The gaps at the wing-sting junctures and spaces above screw heads were filled in with plaster.

Photographs of the damping-in-roll test apparatus are presented in figure 2. The model sting was inserted into the spindle of the rolling-moment balance and secured by a Woodruff key and setscrews. The spindle was rotated at various constant rolling velocities by means of gears and an electric motor outside the tunnel. The rolling velocity was measured with a Stroboconn frequency indicator which was modified to indicate revolutions per minute by means of a generator attached to the rear of the spindle. The rolling moments were measured by strain gages mounted on the spindle downstream of the model and were transmitted through slip rings and brushes to a self-balancing potentiometer outside the tunnel.

TESTS

The damping in roll of three triangular wings was obtained at Mach numbers of 1.62, 1.94, 2.22, 2.41, and 2.62 at nominal angles of attack of 0°, 3.5°, 6.7°, 9.7°, and 12.8°. In each test the angle of attack was corrected for deflections of the models and support system under load. The Reynolds number ranges of the tests, based on the mean aerodynamic chords of the wings, were as follows: 0.92×10^6 to 3.22×10^6 for the wing with $\epsilon = 20^{\circ}$; 0.98×10^6 to 2.41×10^6 for the wing with $\epsilon = 30^{\circ}$; and 0.73×10^6 to 1.82×10^6 for the wing with $\epsilon = 40^{\circ}$. All tests were conducted with transition strips on the wing leading edges in order to insure transition at the same point on the wing surface for all angles of attack and to simulate boundary-layer conditions encountered at higher Reynolds numbers.

The wings and stings were designed so that, when a model was installed in the rolling-moment balance in the tunnel, the roll axis intersected the midchord plane of the wing in the plane of symmetry at the calculated mass center of gravity of the wing.

PRECISION

The maximum probable errors in C_l and $pb/2V$ are given in the following table:

M	Error in C_l	Error in $pb/2V$
1.62	±0.00031	±0.00036
1.94	±.00034	±.00030
2.22	±.00042	±.00023
2.41	±.00021	±.00021
2.62	±.00028	±.00020

The probable errors in C_l may be attributed to errors in the strain-gage indication. The errors in $pb/2V$ were caused by the estimated error in the measurement of the rolling velocity and the surveyed variation of ±0.01 in each of the free-stream Mach numbers.

The angles of attack were accurate to within ±0.1°.

The rolling-moment balance was calibrated statically before and at intervals during the testing to ascertain that there were no changes in the strain-gage constant.

RESULTS AND DISCUSSION

The variations of rolling-moment coefficient with wing-tip helix angle for the three wings tested are presented in figures 3 to 7. Within the accuracy of the data, the values of C_l varied linearly with $pb/2V$. Therefore, the values of C_{l_p}, obtained by taking the slopes of the variations of C_l with $pb/2V$, were, in most instances, independent of rolling velocity.

The variations with angle of attack of the damping in roll of the three wings are presented in figure 8. Within the range of angle of attack of the tests, these variations showed no significant effects of angle of attack on C_{l_p}. However, there was a general trend toward reduced damping with increasing α, especially for the two wings with the higher aspect ratios. The general levels of the variations of damping in roll with α decreased slightly with increasing Mach number. In general, the damping in roll increased with increasing aspect ratio.

However, for the wings of larger aspect ratio, most of the increase in damping with aspect ratio may be attributed to a closer approach to the condition of shock attachment to the leading edge, as will be discussed subsequently.

The experimental and theoretical damping in roll of the wings are compared in figure 9. The experimental values of C_{l_p} are plotted in a manner which allows the theoretical predictions to be represented by a single curve. The abscissa is the quantity $\tan \epsilon/\tan \mu$, which describes the position of the leading edges relative to the Mach cone emanating from the wing apex. Plotted as the ordinate is the quantity βC_{l_p}. The values of βC_{l_p} obtained for the three wings at all five Mach numbers at approximately the same angle of attack are presented in one plot. The theoretical predictions of βC_{l_p} are for isolated wings at zero angle of attack and were obtained from reference 8.

Over the range of $\tan \epsilon/\tan \mu$ of the tests, approximately the same agreement between experiment and theory was obtained for $\alpha \approx 0^\circ$, 3.5°, and 6.7°. (See figs. 9(a), 9(b), and 9(c).) That is, fairly good agreement was obtained when the wing leading edges were well behind the Mach cones ($\tan \epsilon/\tan \mu \lessapprox 0.70$); the damping in roll was generally overestimated by theory when the leading edges were in the vicinity of the Mach cones ($0.70 \lessapprox \tan \epsilon/\tan \mu \lessapprox 1.40$), and the experimental damping in roll was in most instances higher than that predicted by theory when the leading edges were well ahead of the Mach cones ($\tan \epsilon/\tan \mu \gtrapprox 1.40$). Figures 9(d) and 9(e) show that, as the angle of attack was increased to approximately 9.7° and 12.8°, respectively, the damping became less than that of theory when the leading edges were well ahead of the Mach cones ($\tan \epsilon/\tan \mu \gtrapprox 1.40$).

It is interesting to note in figure 9 that, at values of $\tan \epsilon/\tan \mu$ greater than 1.60 for which most of the values of damping were higher than those of theory for $\alpha \approx 0^\circ$, 3.5°, and 6.7° and lower than those of theory for $\alpha \approx 9.7^\circ$ and 12.8°, the leading-edge shock waves were attached for $\alpha \approx 0^\circ$, 3.5°, and 6.7° and were detached for $\alpha \approx 9.7^\circ$ and 12.8°. (For all other experimental values of $\tan \epsilon/\tan \mu$ and α, the leading-edge shock waves were detached.) A decrease in damping might have been expected when the leading-edge shock wave became detached at high angles of attack because of spillage over the leading edge.

The results of the present investigation for $\alpha \approx 0^\circ$ are in fair agreement with the results for triangular wings obtained in references 4, 5, and 6; however, in the present investigation the damping in roll of wings with leading edges well ahead of the Mach cones ($\tan \epsilon/\tan \mu > 1.60$) was higher than theory, whereas it was lower than theory in the investigations of references 5 and 6. The damping in roll of triangular wings

with $\tan \epsilon / \tan \mu > 1.30$ was higher than theory in reference 4. These differences may be due to the fact that, in the investigations of references 5 and 6, the wings were mounted on relatively large bodies of revolution; whereas in the present investigation and in that of reference 4, small mounting stings were used.

CONCLUDING REMARKS

A wind-tunnel investigation of the damping in roll of three triangular wings was made at Mach numbers of 1.62, 1.94, 2.22, 2.41, and 2.62 over a range of angle of attack from approximately 0° to 13°.

Angle of attack had no significant effect on the damping in roll for the range of angles of attack investigated.

For all angles of attack, fairly good agreement between the experimental and theoretical damping in roll was obtained when the wing leading edges were well behind the Mach cones emanating from the wing apexes. When the leading edges were in the vicinity of the Mach cones, the damping in roll was generally overestimated by theory, this overestimation being greater for the higher angles of attack. When the leading edges were well ahead of the Mach cones, the damping in roll varied from somewhat higher than theory for the lower angles of attack to somewhat lower than theory for the higher angles of attack.

Langley Aeronautical Laboratory,
National Advisory Committee for Aeronautics,
Langley Field, Va., May 28, 1956.

REFERENCES

1. McDearmon, Russell W., and Clark, Frank L.: Wind-Tunnel Investigation of the Damping in Roll of the Bell X-1A Research Airplane and Its Components at Supersonic Speeds. NACA RM L55I19, 1956.

2. McDearmon, Russell W., and Clark, Frank L.: Wind-Tunnel Investigation of the Damping in Roll of the Bell X-1E Research Airplane and Its Components at Supersonic Speeds. NACA RM L56B15, 1956.

3. McDearmon, Russell W.: Wind-Tunnel Investigation of the Damping in Roll of the Douglas D-558-II Research Airplane and Its Components at Supersonic Speeds. NACA RM L56F07, 1956.

4. McDearmon, Russell W., and Heinke, Harry S., Jr.: Investigations of the Damping in Roll of Swept and Tapered Wings at Supersonic Speeds. NACA RM L53A13, 1953.

5. Brown, Clinton E., and Heinke, Harry S., Jr.: Preliminary Wind-Tunnel Tests of Triangular and Rectangular Wings in Steady Roll at Mach Numbers of 1.62 and 1.92. NACA RM L8L30, 1949.

6. Bland, William M., Jr., and Sandahl, Carl A.: A Technique Utilizing Rocket-Propelled Test Vehicles for the Measurement of the Damping in Roll of Sting-Mounted Models and Some Initial Results for Delta and Unswept Tapered Wings. NACA TN 3314, 1955. (Supersedes NACA RM L50D24.)

7. Margolis, Kenneth, and Bobbitt, Percy J.: Theoretical Calculations of the Stability Derivatives at Supersonic Speeds for a High-Speed Airplane Configuration. NACA RM L53G17, 1953.

8. Brown, Clinton E., and Adams, Mac C.: Damping in Pitch and Roll of Triangular Wings at Supersonic Speeds. NACA Rep. 892, 1948. (Supersedes NACA TN 1566.)

9. Harmon, Sidney M., and Jeffreys, Isabella: Theoretical Lift and Damping in Roll of Thin Wings With Arbitrary Sweep and Taper at Supersonic Speeds - Supersonic Leading and Trailing Edges. NACA TN 2114, 1950.

10. Malvestuto, Frank S., Jr., Margolis, Kenneth, and Ribner, Herbert S.: Theoretical Lift and Damping in Roll at Supersonic Speeds of Thin Sweptback Tapered Wings With Streamwise Tips, Subsonic Leading Edges, and Supersonic Trailing Edges. NACA Rep. 970, 1950. (Supersedes NACA TN 1860.)

TABLE I

WING DIMENSIONS AND PARAMETERS

Sketch of wing	ϵ, deg	b, in.	c_r, in.	S, sq in.	A
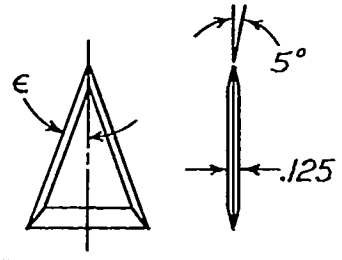	20.0	3.63	4.98	9.02	1.46
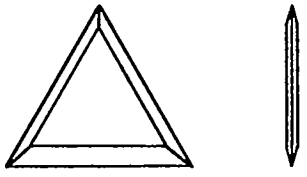	30.0	5.78	5.00	14.43	2.31
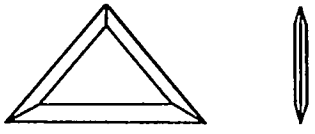	40.0	6.28	3.75	11.76	3.35

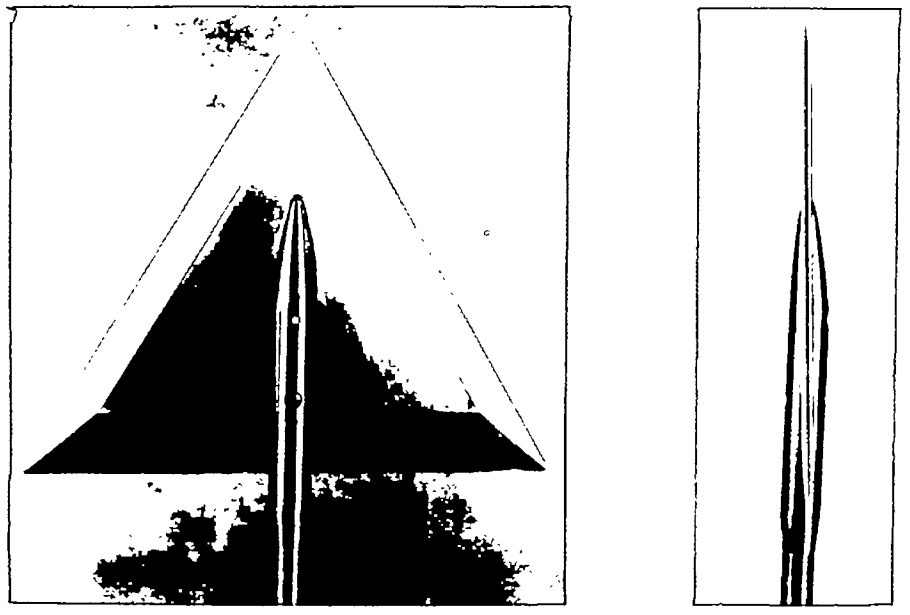

(a) $\alpha \approx 3.5^{\circ}$.

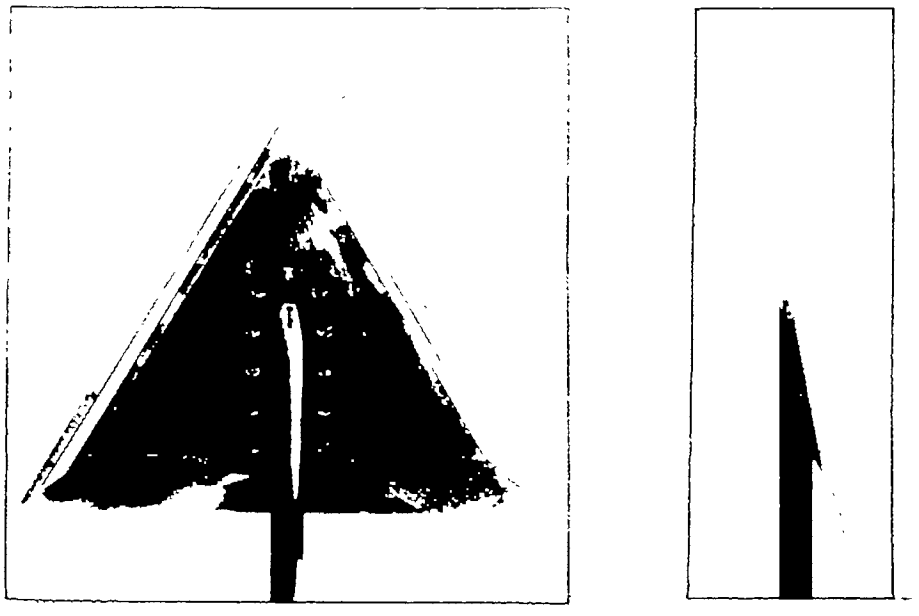

(b) $\alpha \approx 9.7^{\circ}$. L-93529

Figure 1.- Photographs of wings mounted on different types of stings. $\epsilon = 30^{\circ}$.

[redacted]

(a) Test setup in tunnel (top nozzle block removed). L-92300.1

Figure 2.- Photographs of damping-in-roll test apparatus and a typical model.

[redacted]

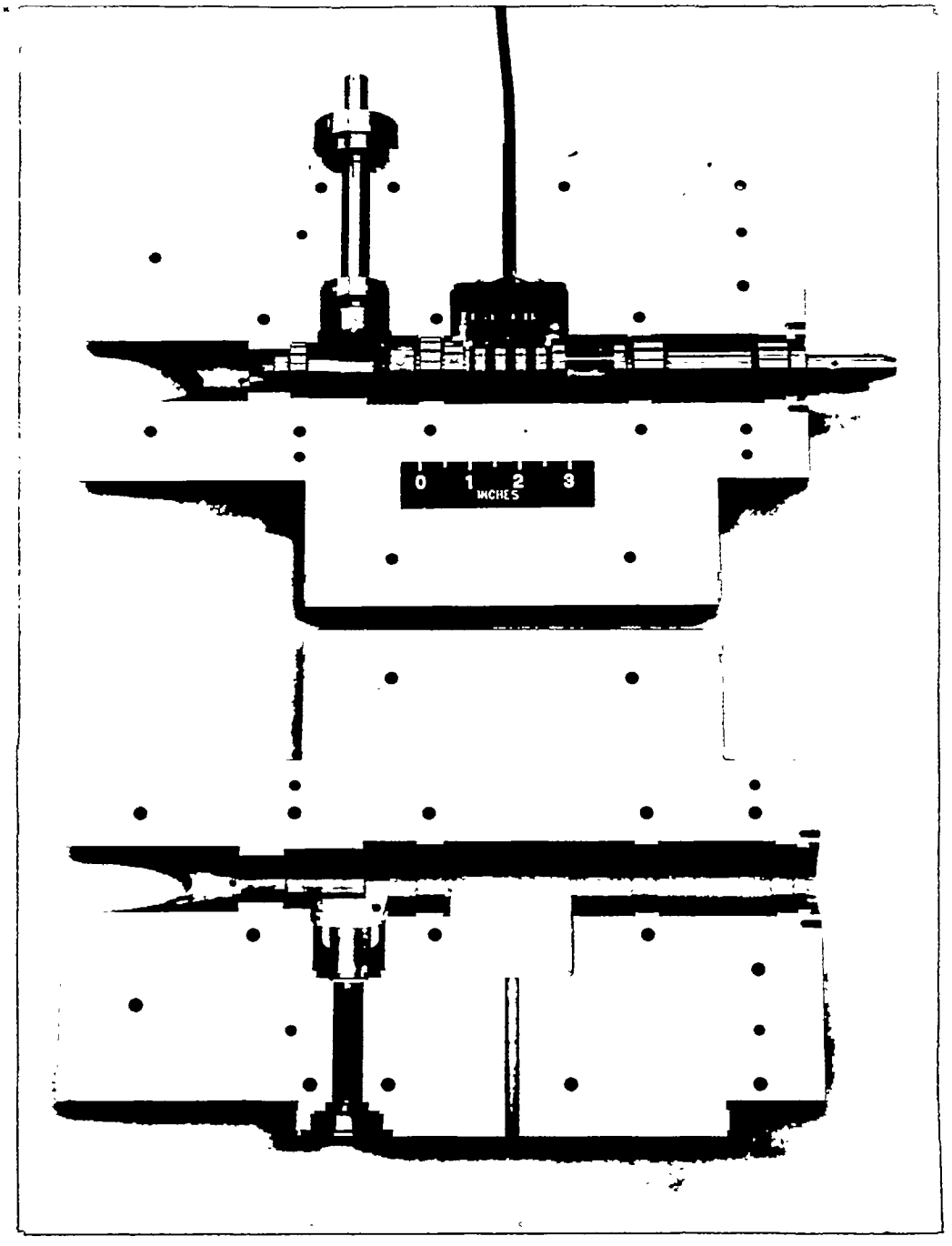

(b) Interior of rolling-moment balance. L-89409

Figure 2.- Concluded.

[redacted]

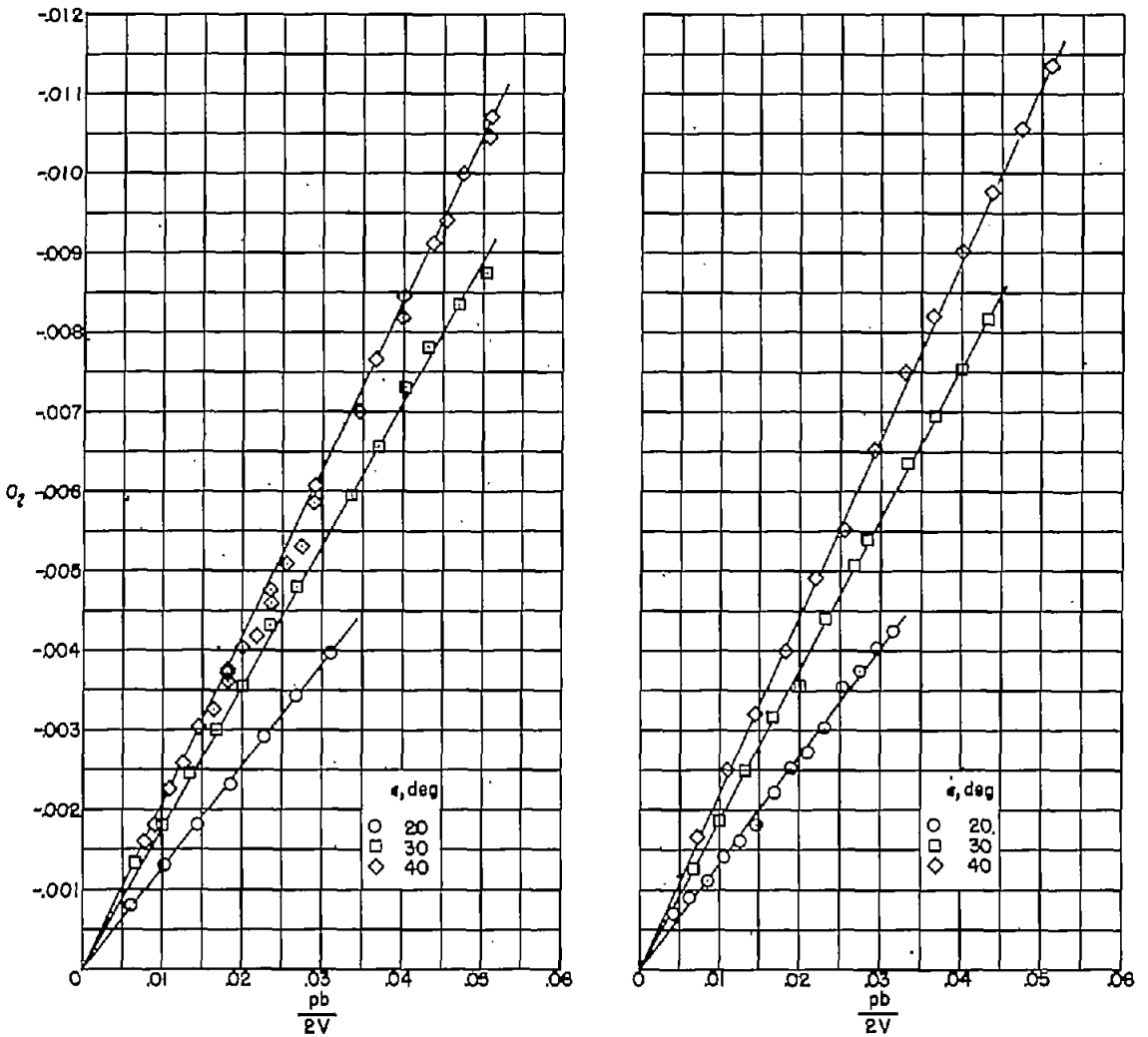

(a) $\alpha \approx 0^{\circ}$.

(b) $\alpha \approx 3.5^{\circ}$.

Figure 3.- Variations of rolling-moment coefficient with wing-tip helix angle at $M = 1.62$.

[redacted]

[redacted]

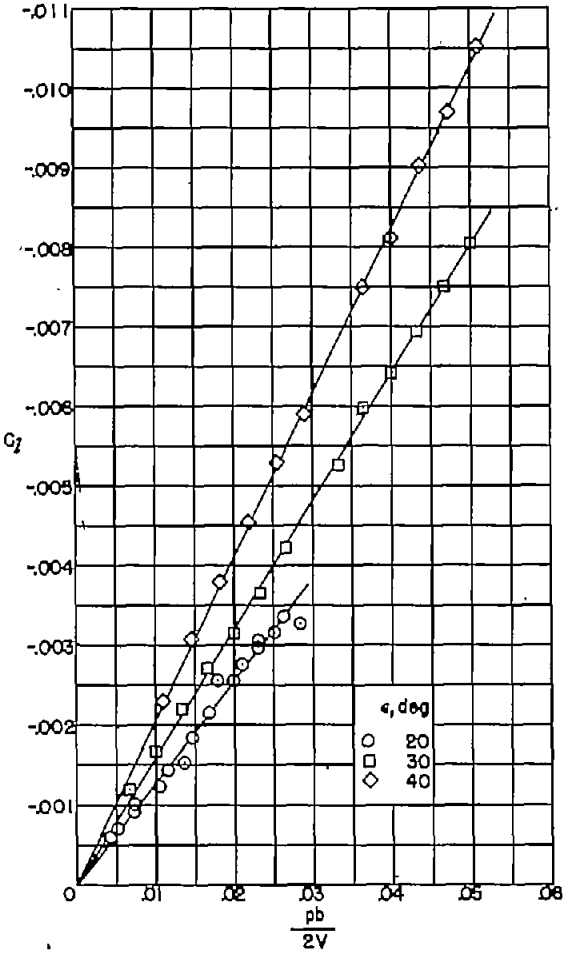

(c) $\alpha \approx 6.7^{\circ}$.

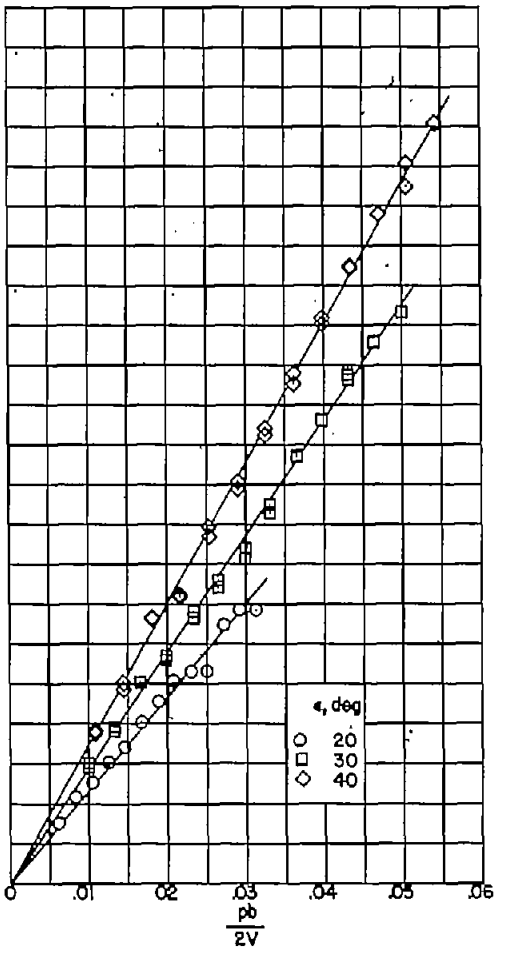

(d) $\alpha \approx 9.7^{\circ}$.

Figure 3.- Continued.

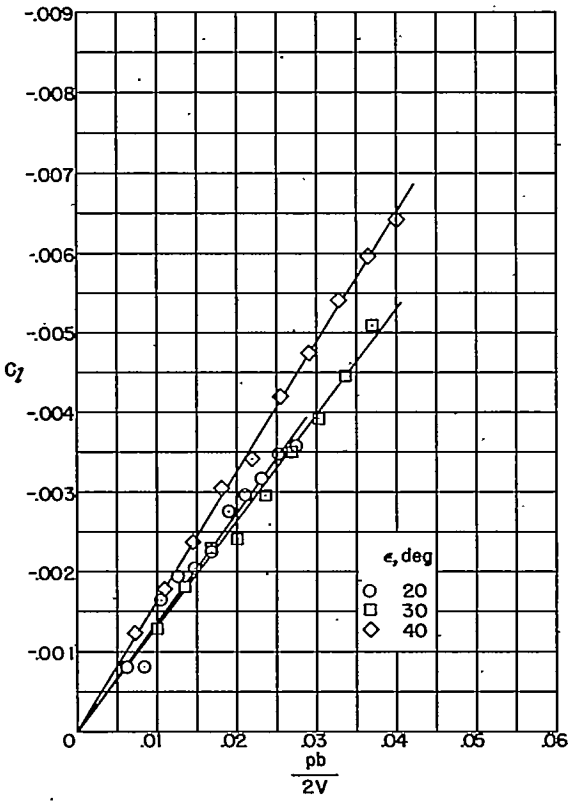

(e) $\alpha \approx 12.8^{\circ}$.

Figure 3.- Concluded.

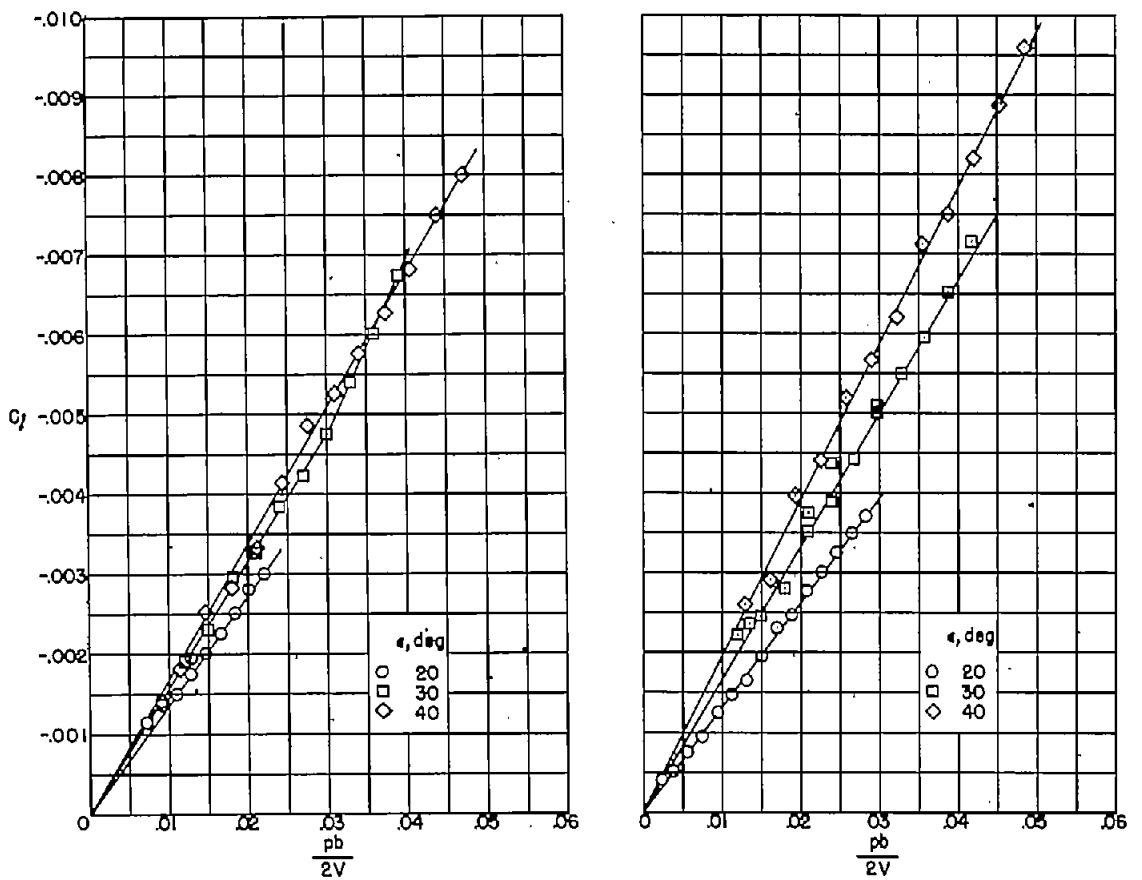

(a) $\alpha \approx 0^{\circ}$.

(b) $\alpha \approx 3.5^{\circ}$.

Figure 4.- Variations of rolling-moment coefficient with wing-tip helix angle at $M = 1.94$.

[redacted]

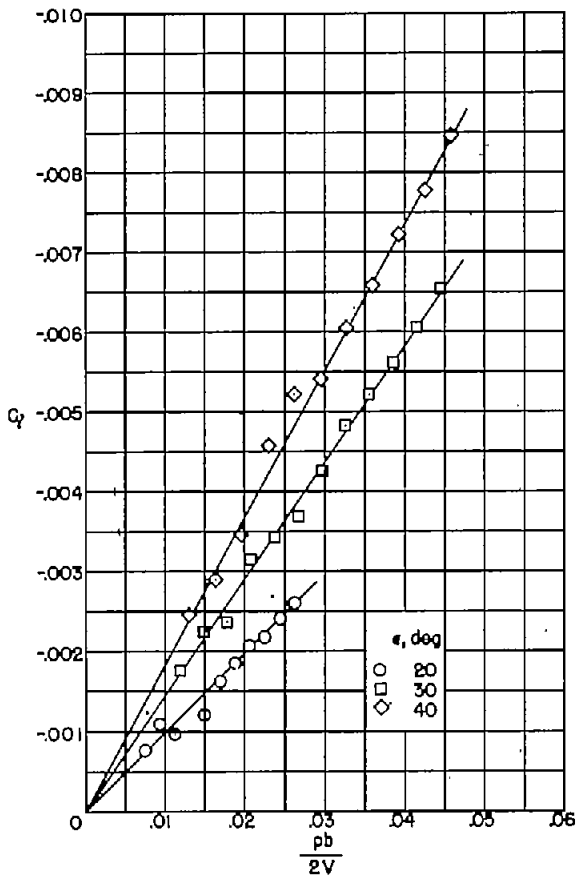

(c) $\alpha \approx 6.7^{\circ}$.

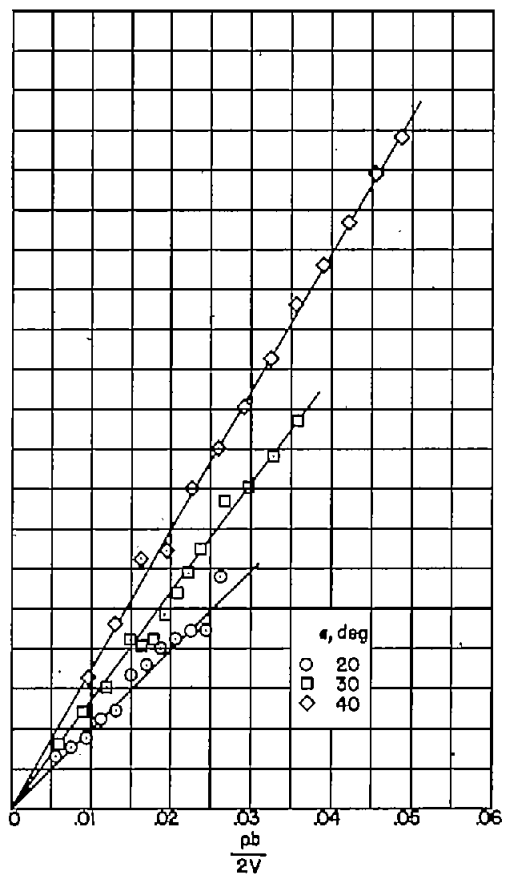

(d) $\alpha \approx 9.7^{\circ}$.

Figure 4.- Continued.

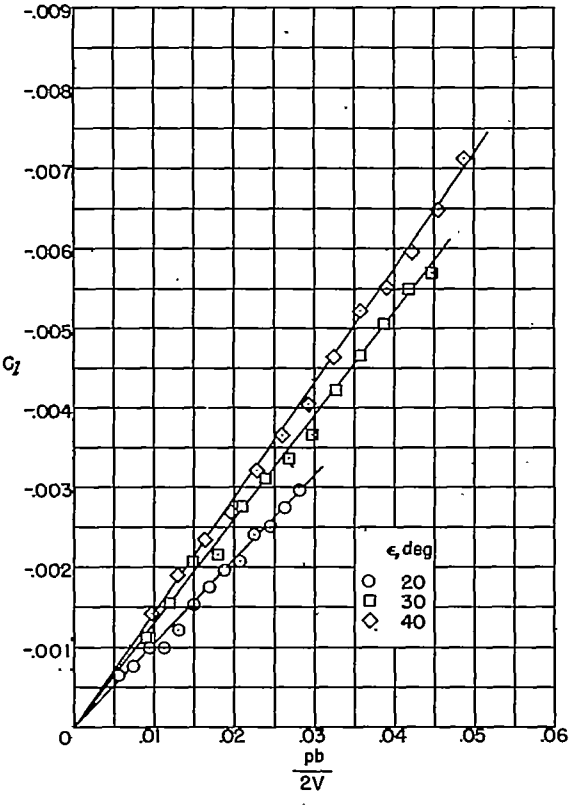

(e) $\alpha \approx 12.8^{\circ}$.

Figure 4.- Concluded.

[redacted]

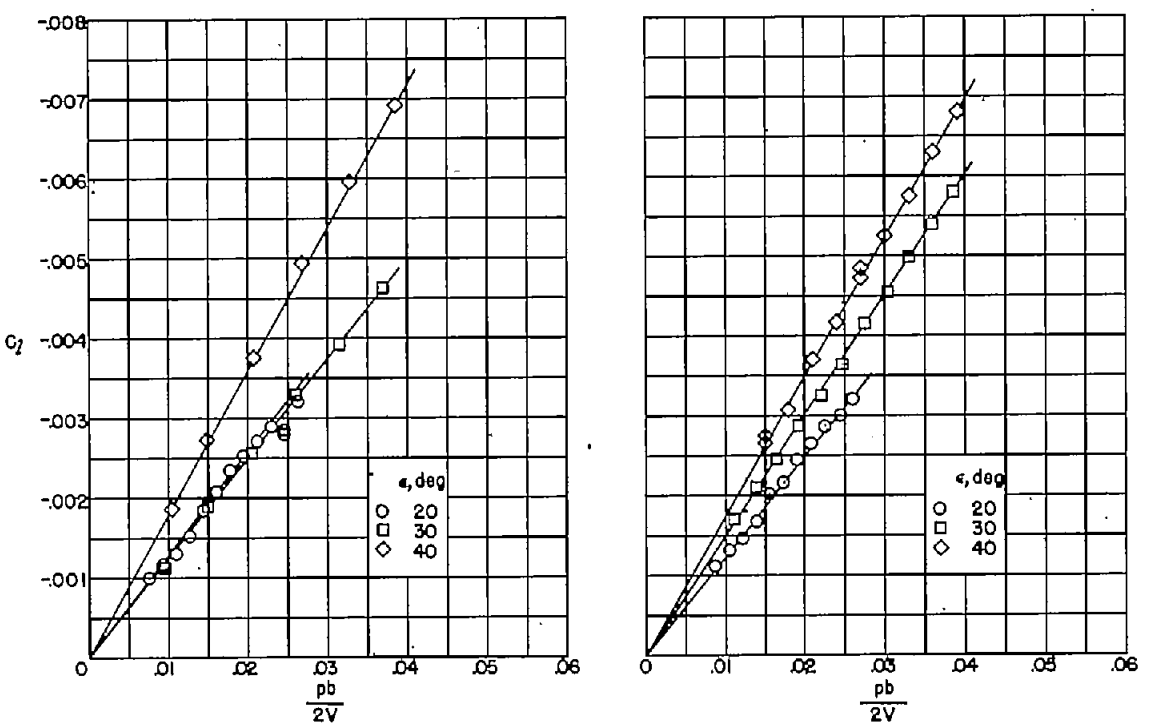

(a) $\alpha \approx 0^{\circ}$.

(b) $\alpha \approx 3.5^{\circ}$.

Figure 5.- Variations of rolling-moment coefficient with wing-tip helix angle at $M = 2.22$.

[redacted]

[redacted]

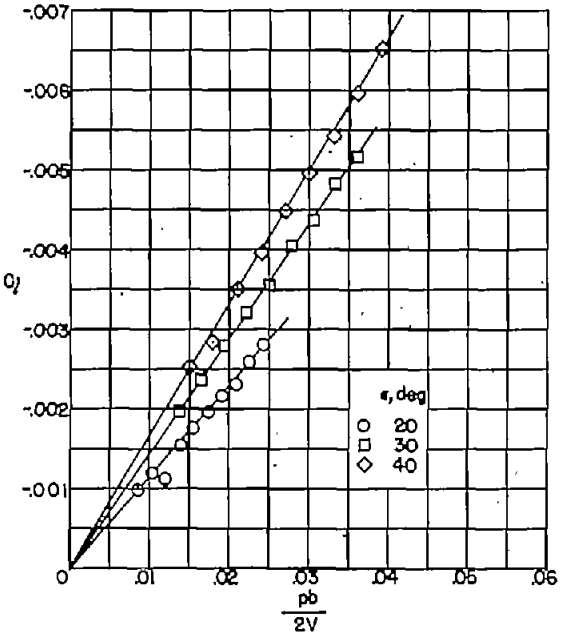

(c) $\alpha \approx 6.7^{\circ}$.

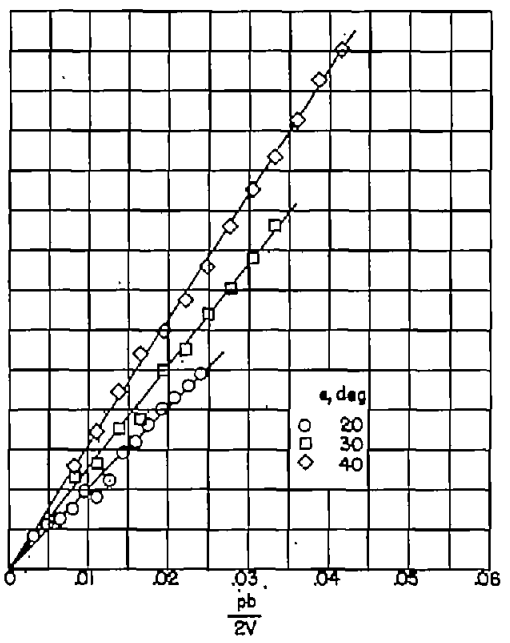

(d) $\alpha \approx 9.7^{\circ}$.

Figure 5.- Continued.

[redacted]

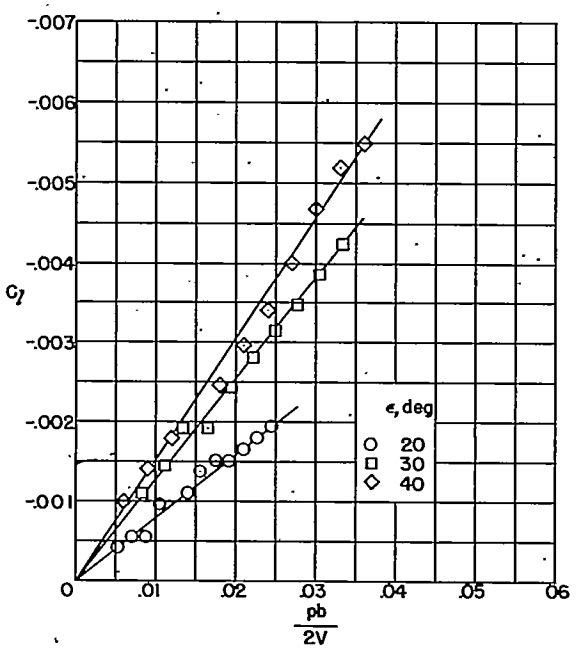

(e) $\alpha \approx 12.8^{\circ}$.

Figure 5.- Concluded.

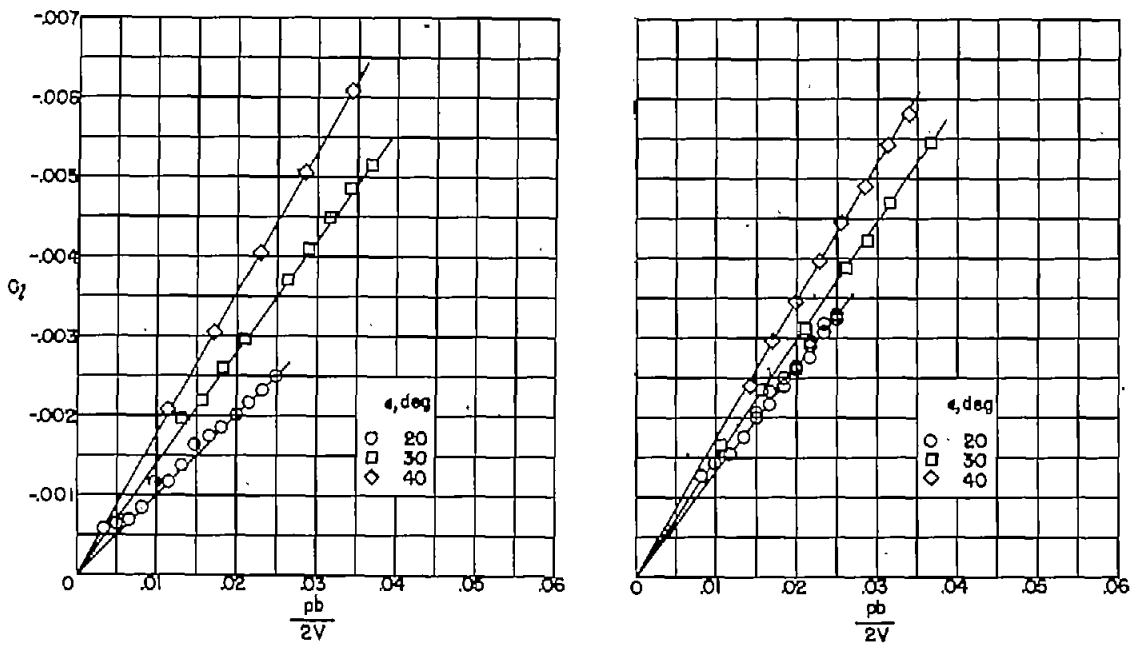

(a) $\alpha \approx 0^{\circ}$.

(b) $\alpha \approx 3.5^{\circ}$.

Figure 6.- Variations of rolling-moment coefficient with wing-tip helix angle at $M = 2.41$.

[redacted]

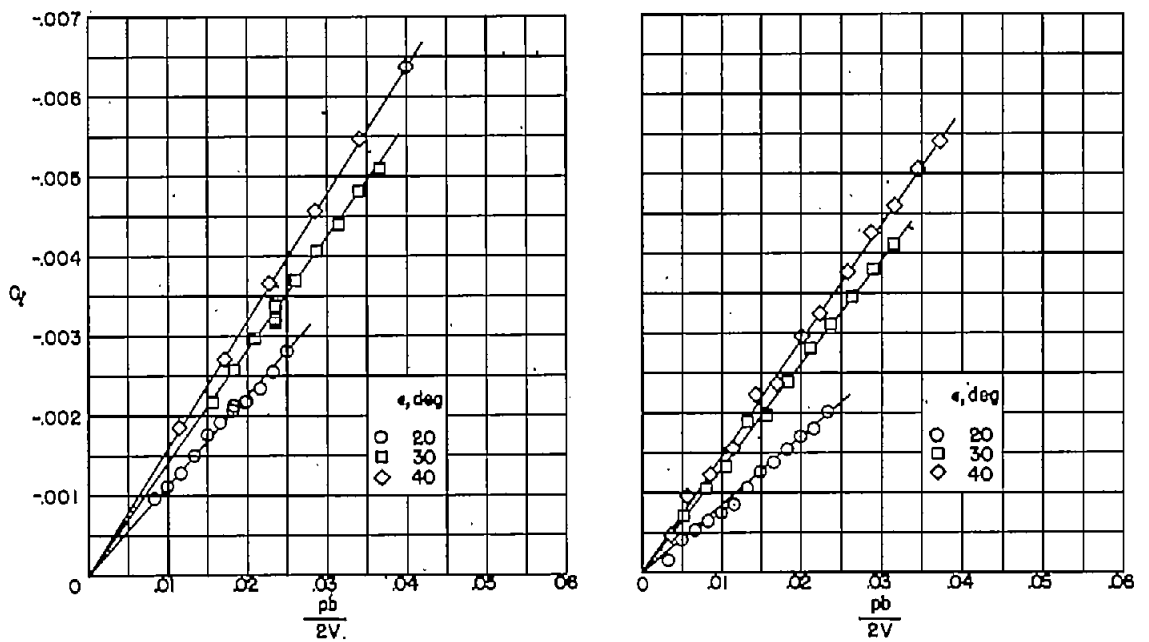

(c) $\alpha \approx 6.7^{\circ}$.

(d) $\alpha \approx 9.7^{\circ}$.

Figure 6.- Continued.

[redacted]

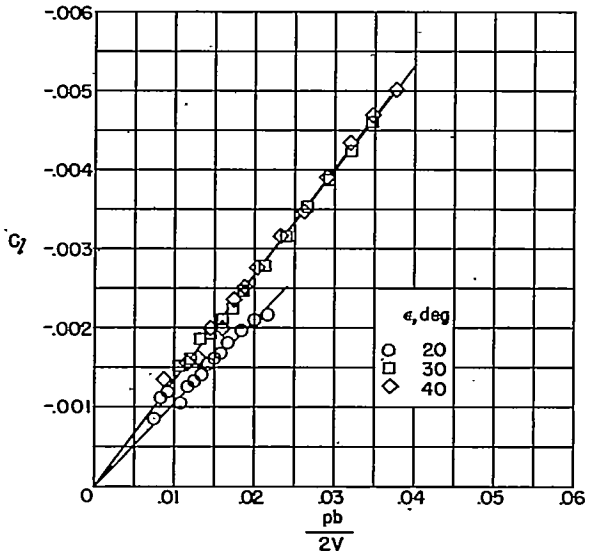

(e) $\alpha \approx 12.8^{\circ}$.

Figure 6.- Concluded.

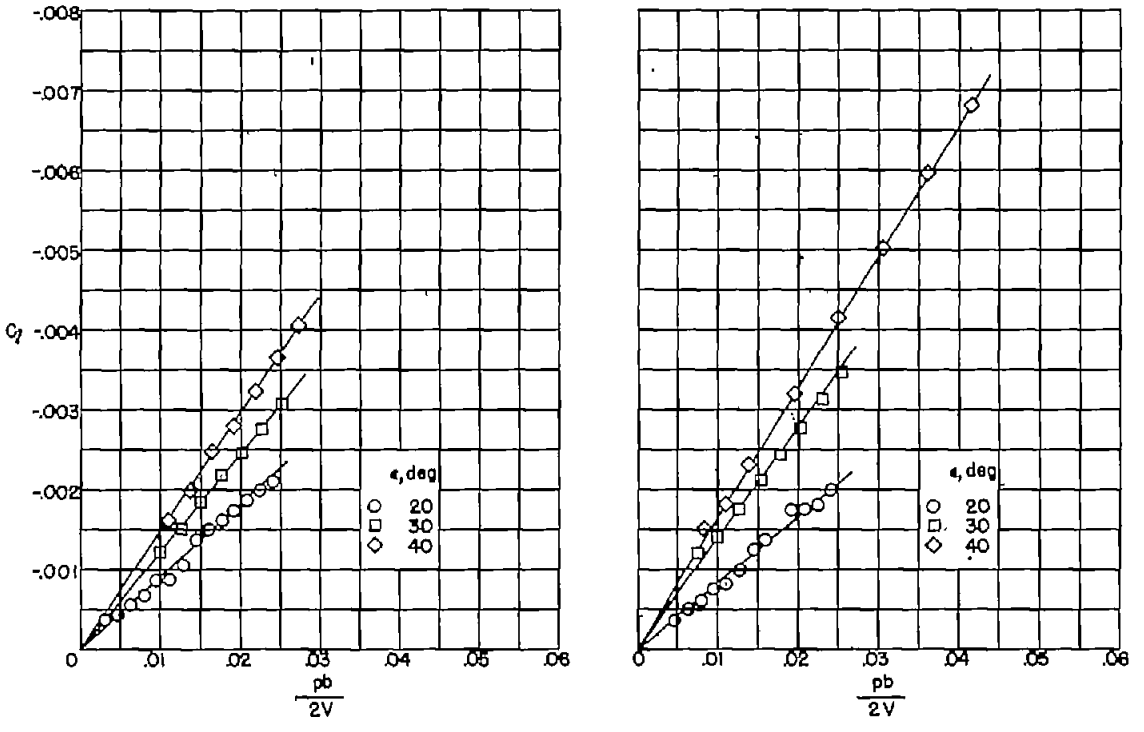

(a) $\alpha \approx 0^{\circ}$.

(b) $\alpha \approx 3.5^{\circ}$.

Figure 7.- Variations of rolling-moment coefficient with wing-tip helix angle at $M = 2.62$.

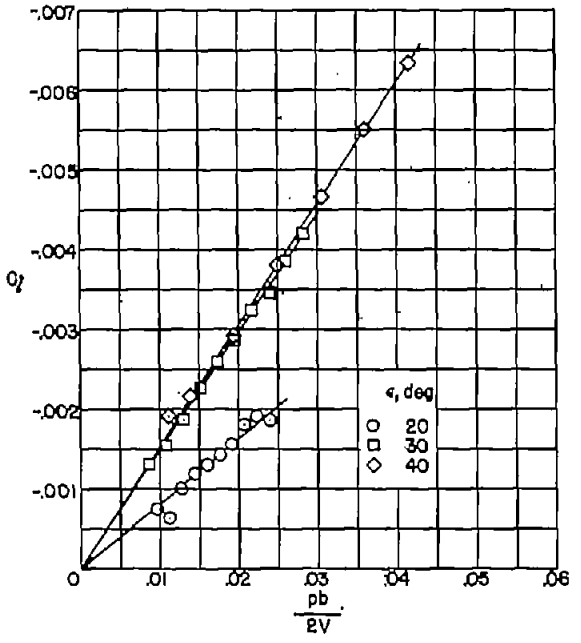

(c) $\alpha \approx 6.7^{\circ}$.

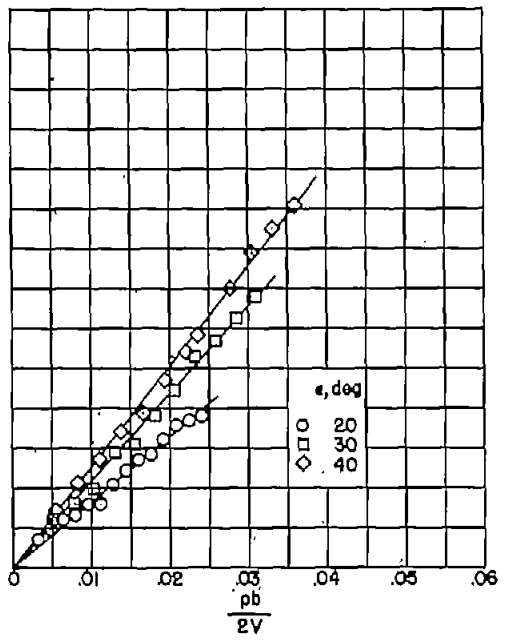

(d) $\alpha \approx 9.7^{\circ}$.

Figure 7.- Continued.

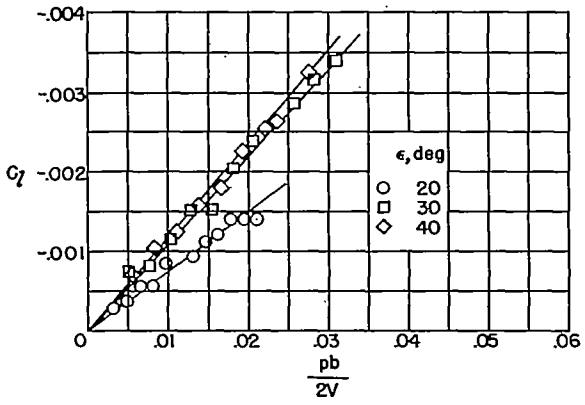

(e) $\alpha \approx 12.8^{\circ}$.

Figure 7.- Concluded.

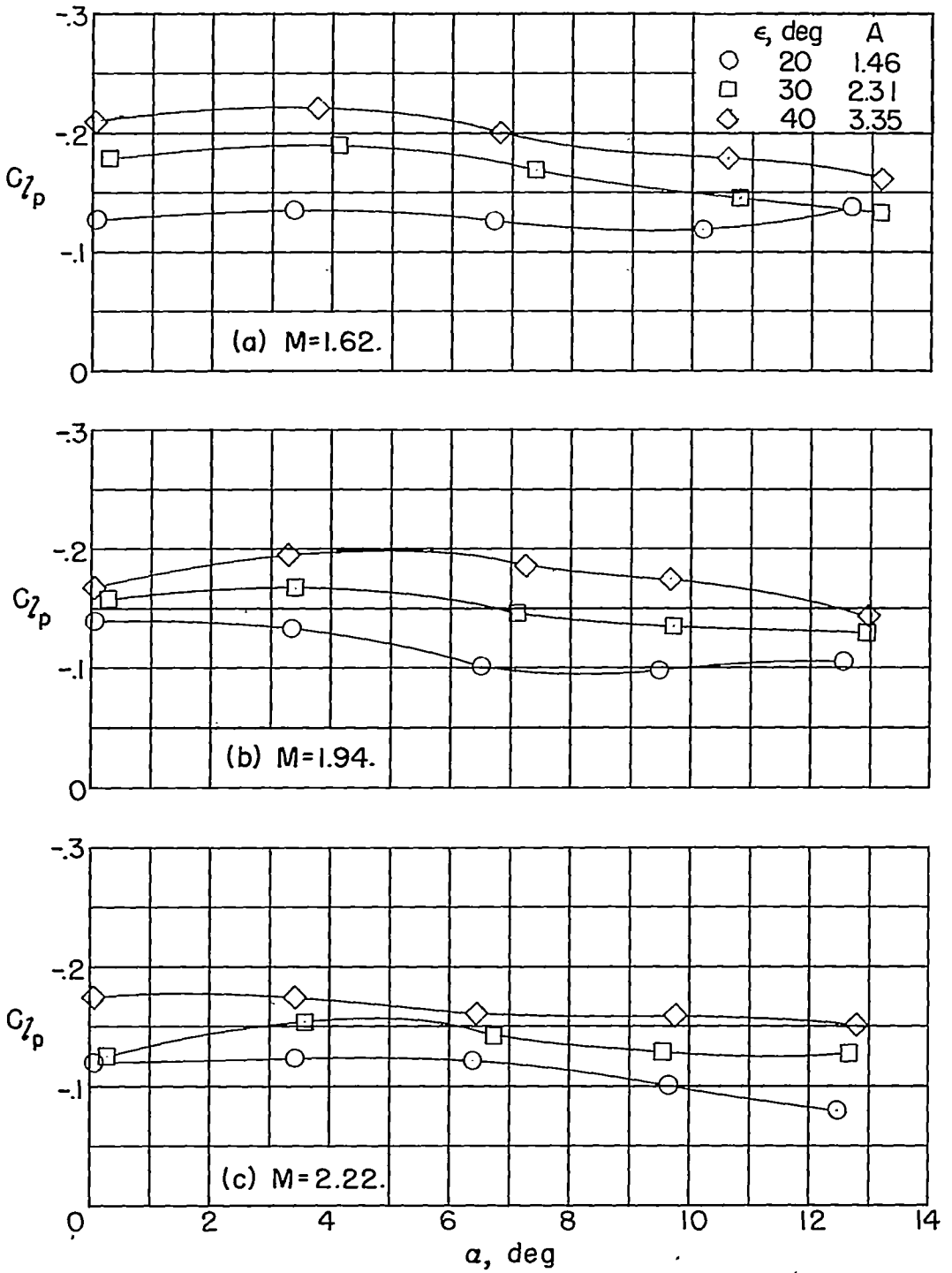

Figure 8.- Variations with angle of attack of damping in roll of the three wings.

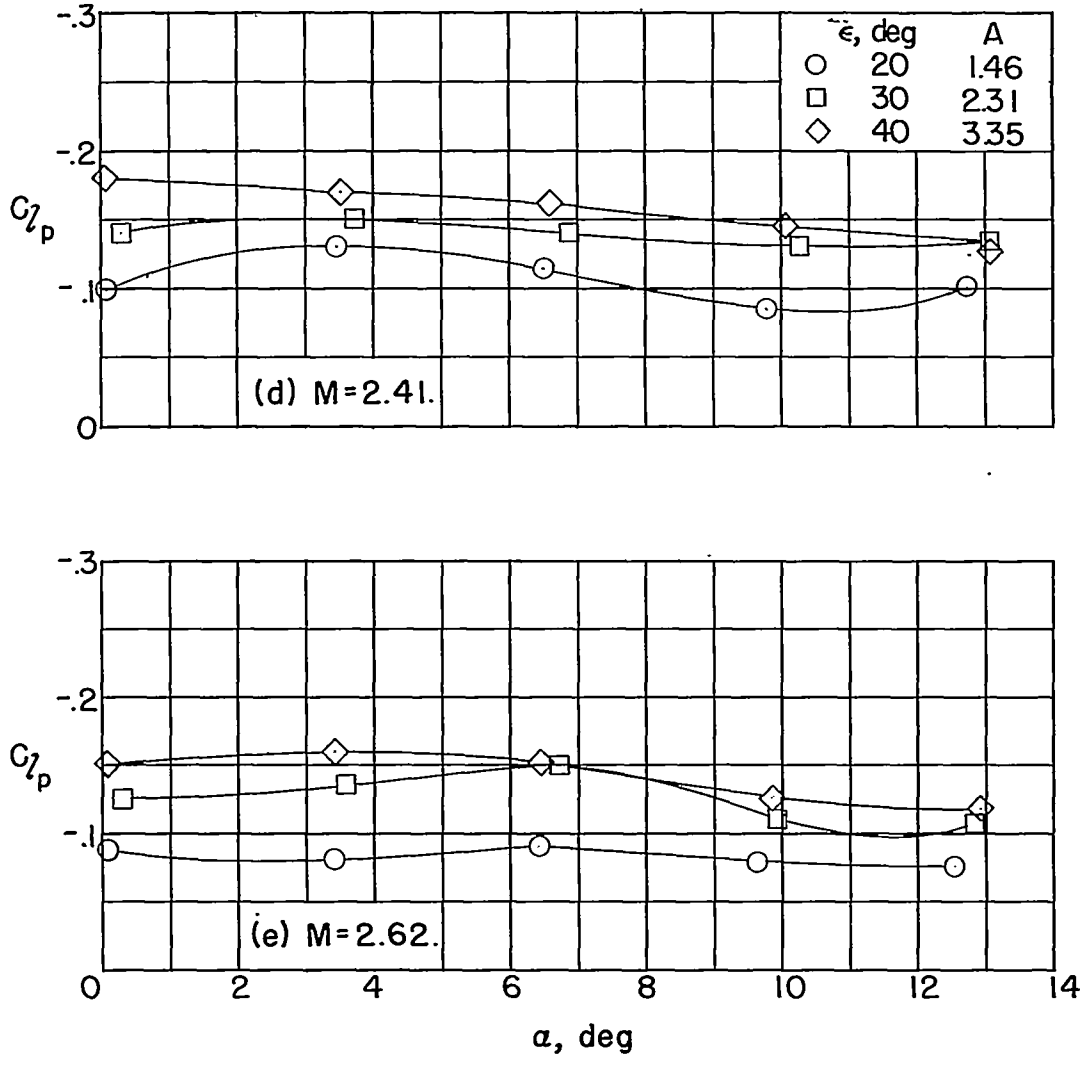

Figure 8.- Concluded.

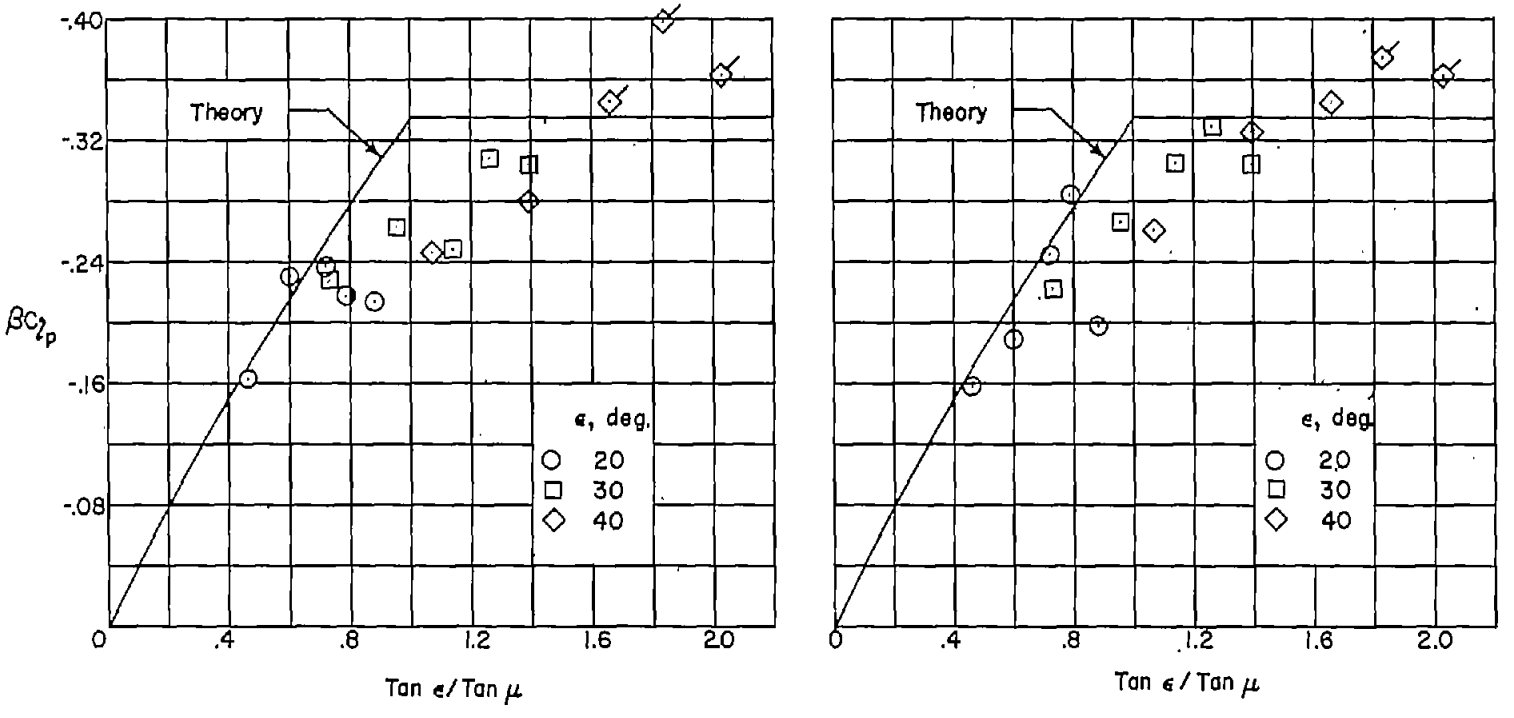

(a) $\alpha \approx 0^{\circ}$.

(b) $\alpha \approx 3.5^{\circ}$.

Figure 9.- Comparison of experimental and theoretical damping in roll of the three wings. Flagged symbols denote points for which the leading-edge shock waves were attached.

[redacted]

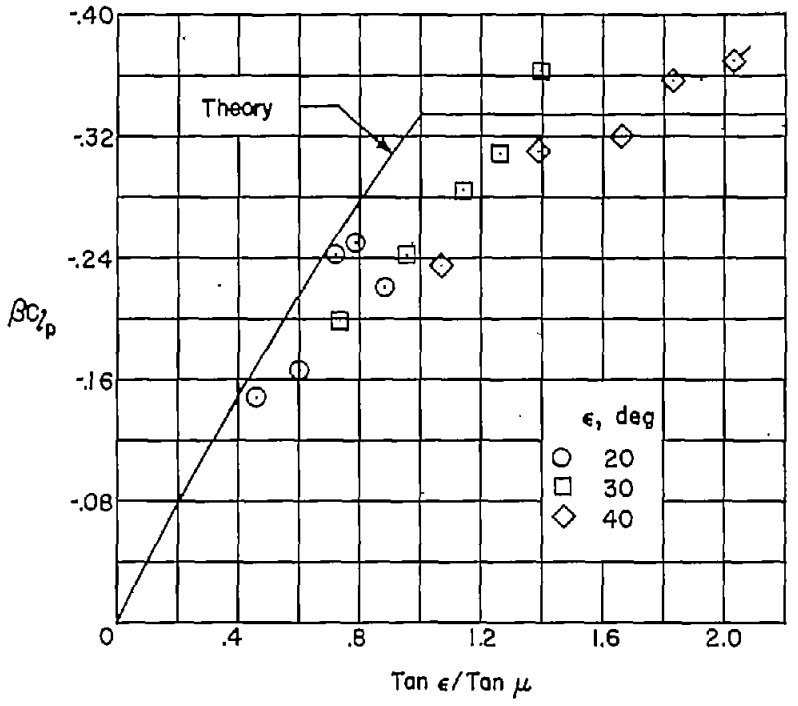

(c) $\alpha \approx 6.7^{\circ}$.

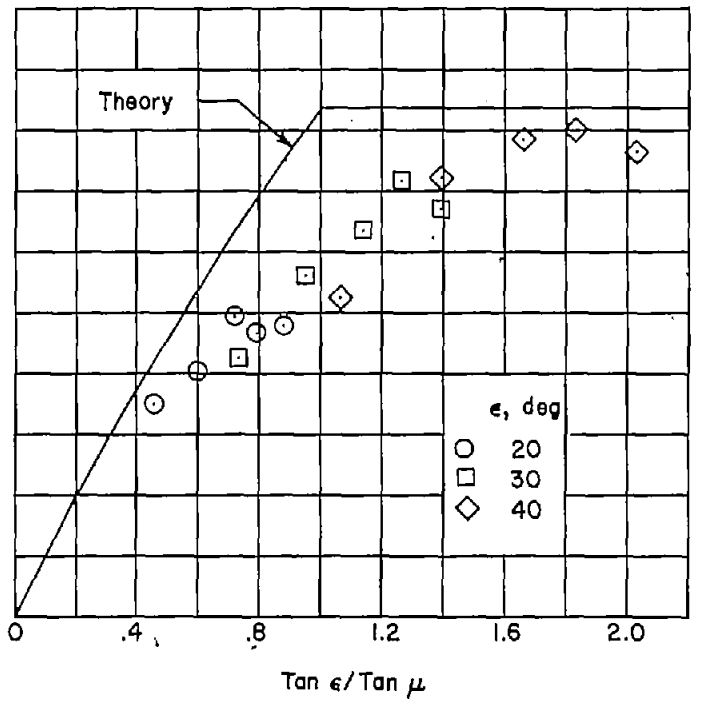

(d) $\alpha \approx 9.7^{\circ}$.

Figure 9.- Continued.

[redacted]

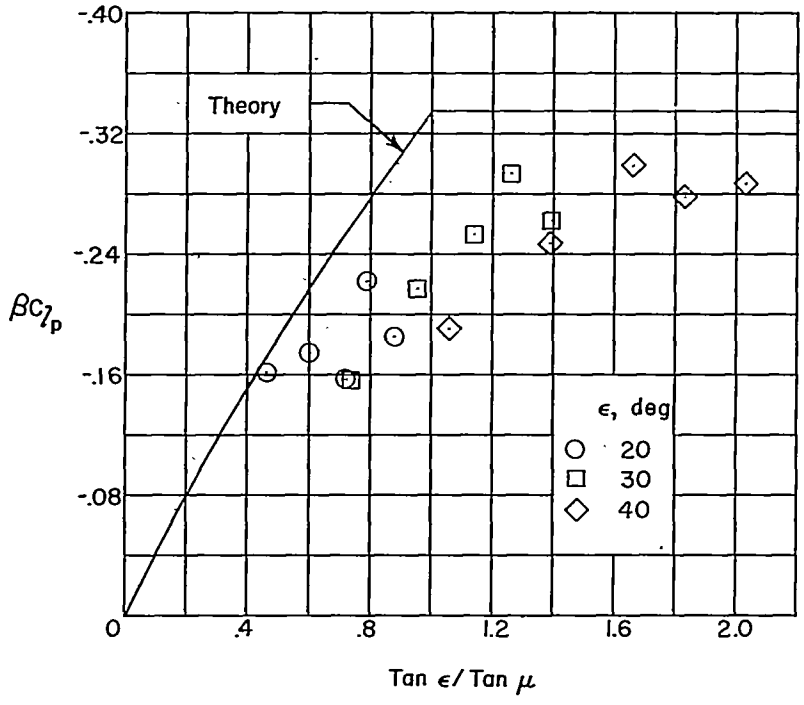

(e) $\alpha \approx 12.8^{\circ}$.

Figure 9.- Concluded.